Intermolecular Forces in van der Waals Complexes between Argon and Aromatic Molecules: Rotational Spectrum and ab Initio Investigation of Isoxazole−Argon

U. Spoerel, H. Dreizler, and W. Stahl*,†

Abteilung Chemische Physik, Institut für Physikalische Chemie, Christian-Albrechts-Universität, D-24098 Kiel, Germany

Elfi Kraka* and Dieter Cremer

Department of Theoretical Chemistry, University of Göteborg, Kemigården 3, S-42296 Göteborg, Sweden

Received: February 27, 1996; In Final Form: May 24, 1996[⊗]

The rotational spectrum of the isoxazole−argon complex was studied in the microwave region between 3 and 25 GHz using a pulsed molecular beam Fourier transform microwave spectrometer. The rotational constants were found to be $A = 4974.2534(2)$ MHz, $B = 1382.291\,788(24)$ MHz, and $C = 1371.647\,236(36)$ MHz. The centrifugal distortion constants are $D'_J = 5.624\,21(30)$ kHz, $D'_K = -27.8794(256)$ kHz, $D'_{JK} = 34.8064(34)$ kHz, $\delta'_J = -0.010\,48(24)$ kHz, and $R'_6 = -0.000\,40(18)$ kHz. The diagonal elements and one off-diagonal element of the quadrupole coupling tensor were determined to be $\chi_{aa} = -0.113\,10(48)$ MHz, $\chi_{bb} = 1.941\,36(87)$ MHz, $\chi_{cc} = -1.828\,26(45)$ MHz, and $\chi_{bc} = \pm 4.8954(22)$ MHz. Using BSSE-corrected supermolecular Møller−Plesset (MP) perturbation theory at second (MP2) and fourth order (MP4(SDTQ)) with a (14s10p2d1f)[7s4p2d1f] basis set for argon and a 6-31G(+sd+sp) basis for isoxazole, stability (MP2 308 cm^{-1}; MP4 283 cm^{-1}), equilibrium geometry, charge distribution, and multipole moments of the complex were determined. Argon adopts a position above the ring plane (Ar−ring distance $R = 3.44$ (exp), 3.53 (MP2, r_e), 3.55 Å (MP4, r_e) shifted from the center of the ring toward the NO bond. The complex is predominantly stabilized by dispersion interactions while its geometry is more a result of exchange repulsion forces, which direct Ar toward the most electronegative atoms of the ring, namely O and N.

1. Introduction

Isoxazole plays an important role in biology and pharmacology,[1] which is reflected by the fact that, e.g., its sulfisoxazoles derivatives are used as antibiotics. Because of this, there is a need to understand structure, stability, reactivity, and other molecular properties of the molecule. Some work has been carried out to this extent[2−4] and there is general knowledge about its molecular structure and stability. However, less is known how isoxazole behaves at the onset of a chemical reaction. This work makes a contribution to this question by investigating the van der Waals complex between isoxazole and argon.

The investigation of van der Waals complexes leads to an understanding of the forces that act between molecules in bulk matter and, therefore, provides a first insight into the reactivities of the complex partners.[5] Van der Waals complexes involving argon atoms are a particularly rewarding research goal since a noble gas atom does not possess any permanent electric multipole moments.[6] Accordingly, the binding energy of an Ar van der Waals complex such as isoxazole−argon is determined by the induction energy E^{in} caused by the interaction of the permanent electric multipole moments of isoxazole with the electric multipole moments induced in Ar, then the dispersion energy E^{dis} which is caused by the mutual polarization of the electron density of the two complex partners (interactions of the instantaneous multipoles which are related to dynamic multipole polarizabilities), and, finally, the exchange repulsion (overlap repulsion) energy E^{es} as a result of the Pauli principle, which prevents electrons of isoxazole from penetrating into the occupied space of Ar.[7] The fourth type of interactions, namely the electrostatic interactions between permanent electric multipole moments of the complex partners, is absent in the case of an Ar van der Waals complex, which considerably facilitates the investigation of the forces between the complex partners.[6]

Because of its spherical electron density distribution, Ar can be considered as a structureless probe for the electronic properties of that molecule Ar is bound to in a van der Waals complex. Investigation of the latter leads to a description of the polarizability and reactive behavior of the partner molecule. Numerous investigations of Ar van der Waals complexes have exploited this aspect as is amply documented in the literature.[5,6] Recently, research has focused on Ar van der Waals complexes that involve aromatic partner molecules such as benzene−argon,[8] fluorobenzene−argon,[9] 1,2,4,5-tetrafluorobenzene−argon,[10] pyridine−argon,[11] furan−argon,[12] pyrrole−argon,[13] or oxazole−argon.[14] For symmetric partner molecules such as benzene[8] or 1,2,4,5-tetrafluorobenzene,[10] Ar is located above the center of the aromatic ring while it is shifted in an off-center position if the benzene ring is asymmetrically substituted as in fluorobenzene−argon[9] or replaced by a heteroaromatic system of lower symmetry.[11−13] The exact position of the Ar atom reflects the distribution of the π-electrons in the aromatic ring and provides insight into the various modes of attack by an electron-rich partner.

Investigation of Ar van der Waals complexes involving heteroaromatic systems are particularly interesting in this connection, which caused us to study complexes such as oxazole−argon[14] or isoxazole−argon. Recently, we have described the oxazole−argon van der Waals complex by employing molecular beam (MB) Fourier transform microwave (FTMW) spectroscopy and high-level ab initio theory.[14] In this investigation we developed a model for Ar van der Waals complexes that can explain measured properties of investigated

† Present address: Institut für Physikalische Chemie, RWTH Aachen, Templergraben 59, D-52056 Aachen, Germany.

⊗ Abstract published in *Advance ACS Abstracts,* July 15, 1996.

S0022-3654(96)00600-4 CCC: $12.00

complexes and, in addition, can be used for predicting the properties of Ar complexes so far not investigated by MW spectroscopy. For example, for the oxazole−argon complex this model predicts an equilibrium geometry, in which the Ar atom is located above the ring plane shifted toward the O atom.

In this work, we investigate the isoxazole−argon complex by a two-pronged approach: First, we report the rotational spectrum measured with a molecular beam (MB) Fourier transform microwave spectrometer (FTMW) at a very low rotational temperature. This investigation leads to four possible complex geometries of which two seem to be more likely to represent the most stable geometry of the complex. Further distinction is not possible on the basis of the experimental data currently available and, therefore, the identification of the most stable complex geometry has to be based on ab initio calculations.

In the second part of this work, we present an ab initio investigation carried out with supermolecular Møller−Plesset (MP) perturbation theory[15] at first (MP1 = Hartree−Fock (HF)), second (MP2), third (MP3), and fourth order (MP4) with basis sets especially designed for studies of argon containing van der Waals complexes. These calculations lead to a characterization of the most stable configuration and a description of the forces between the argon atom and the isoxazole ring. Finally, we will verify the predictive power and usefulness of the model developed previously.[14]

In the following, we present results of the FTMW measurements (section 2), a summary of calculational procedures and results (section 3), and a discussion of complex geometry, complex stability, and the intermolecular forces stabilizing and destabilizing isoxazole−argon (section 4).

2. Experimental Section

The investigation of isoxazole−argon by means of a MB-FTMW spectrometer was performed at a very low rotational temperature. The isoxazole−argon complex was found to be a nearly prolate top like oxazole−argon. The rotational constants and the quadrupole coupling tensor were determined using least-squares fits. The strong disturbance in the hyperfine structure was analyzed to be due to the element χ_{bc} of the quadrupole coupling tensor. We tried to determine the complex geometry using rotational constants and the appropriately rotated dipole moment vector of isoxazole with the help of spectra obtained in the scanning mode.

All spectra were taken using our MB-FTMW spectrometer[16] in the range from 3 to 25 GHz. For highest resolution and sensitivity the nozzle was mounted in such a way that the molecular beam propagates along the axis of the cavity from one mirror to the other.[17] Gas mixtures containing 1% isoxazole (Aldrich, Steinheim) in argon and a stagnation pressure of 50−75 kPa were used throughout.

2.1. Spectral Analysis. We started our investigation by predicting rotational constants. Therefore, we assumed the geometry of isoxazole to remain unchanged upon complexation and the argon atom located 3.5 Å above the center of the ring. Using the isoxazole geometry given by Stiefvater, Sheridan, and Nösberger,[2] we predicted the rotational constants and calculated transitions. In the same way as done for oxazole−argon, we first predicted *a*-, *b*-, and *c*-type spectrum for the complex due to a dipole moment vector in the principal axis system of isoxazole−argon obtained by rotation of the dipole moment vector measured by Stiefvater.[3] We started our search by scanning the range from 3710 to 3480 MHz. Twelve lines were found and assumed to form a Q-branch. They vanished when

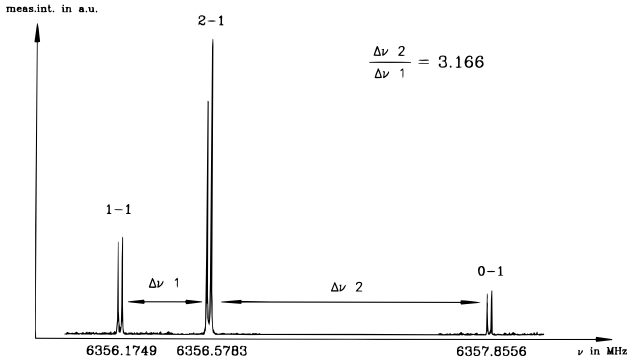

Figure 1. $J_{KaKc} = 1_{10}-0_{00}$ transition of isoxazole−argon. Amplitude spectrum composed of three single spectra, each recorded with 8K Fourier transformation, 1024−3584 cycles at the given polarization frequencies.

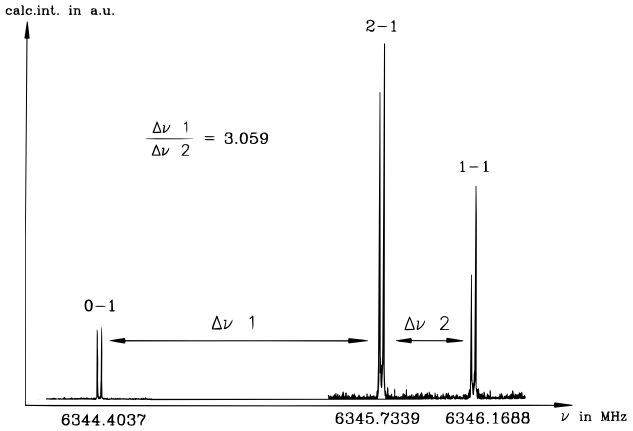

Figure 2. $J_{KaKc} = 1_{11}-0_{00}$ transition of isoxazole−argon. Amplitude spectrum composed of three single spectra, 8K Fourier transformation, 1024−2048 cycles at the given polarization frequencies.

helium was used as a carrier gas. A least-squares fit yielded two improved rotational constants. With a new prediction the two $J = 1-0$ transitions and 32 more lines belonging to Q- and P-branches could be found. Since isoxazole has a nitrogen nucleus, a hyperfine structure was observed. The hyperfine structure of the two $J = 1-0$ transitions is strongly disturbed as can be seen in Figures 1 and 2. Usually the ratio of the splittings of the hyperfine structure is here 1.5. It was found that the disturbance, which is only seen that strongly in the two $J = 1-0$ transitions, is due to the element χ_{bc} of the quadrupole coupling tensor.

All lines were of *b* or *c* type. In the course of the calculation of the geometry of isoxazole−argon, we also predicted *a*-type transitions. As a consequence, seven additional lines of *a* type with 20 components were found. All measured lines are listed in Table 1. The rotational, quartic centrifugal distortion constants according van Eijck,[18] the diagonal elements as well as one off-diagonal element of the quadrupole coupling tensor, and the highest correlation coefficient are presented in Table 2. All spectroscopic constants were determined using least-squares fits. The freedom−cofreedom matrix[19] indicates a satisfactory fit of the rotational parameters.

In the course of our studies we also remeasured transitions of isoxazole in order to determine the quadrupole tensor of isoxazole more precisely by analyzing the hyperfine splittings. Since isoxazole is a planar molecule, two off-diagonal elements of the quadrupole coupling tensor, χ_{ac} and χ_{bc}, are zero. The third off-diagonal element, χ_{ab}, is very large and the magnitude could be determined without measurements of isotopomers. This was possible since χ_{ab} causes noticeable deviations in the

TABLE 1: Observed Transitions of Isoxazole−Argon

$J''K_a''K_c''-J'K_a'K_c'$	F″−F′	obs (MHz)	obs − calc (kHz)	$J''K_a''K_c''-J'K_a'K_c'$	F″−F′	obs (MHz)	obs − calc (kHz)
100−000	2−1	6356.5783	0.3	413−404	5−5	3650.3097	1.3
	1−1	6356.1749	−0.9		4−4	3649.6781	0.8
	0−1	6357.8556	−0.9		3−3	3650.4808	1.0
111−000	2−1	6345.7339	0.1	414−404	5−5	3543.5092	0.8
	1−1	6346.1688	−0.8		4−4	3544.1389	1.2
	0−1	6344.4037	−1.0		3−3	3543.3400	1.3
110−101	2−2	3602.6561	0.4	422−413	5−5	10737.1796	1.2
	2−1	3602.6910	1.2		4−4	10737.8183	0.8
	1−2	3602.2529	−0.7		3−3	10737.0057	0.8
	1−0	3602.2028	0.3	423−413	5−5	10736.8224	1.4
	1−1	3602.2876	−0.1		4−4	10737.4687	1.0
111−101	1−1	3592.2818	0.3		3−3	10736.6470	0.9
	1−2	3592.2469	−0.5	505−414	6−5	10222.9014	0.3
	1−0	3592.1969	0.6		5−4	10222.2750	−0.1
	2−1	3591.8469	0.3		4−3	10223.0658	−0.6
	2−2	3591.8119	0.3	505−413	6−5	10116.1013	0.3
	0−1	3590.5163	−0.3		5−4	10116.7356	0.2
212−101	3−2	9088.6939	0.1		4−3	10115.9251	−0.2
	2−2	9089.2359	−0.1	515−404	6−5	17283.3163	1.4
	2−1	9089.2707	−0.4		5−4	17283.9582	1.1
	1−1	9088.3586	−1.6		4−3	17283.1794	0.7
	1−0	9088.2744	−0.6	514−404	6−5	17443.3677	1.3
211−101	3−2	9120.9047	−0.3		5−4	17442.7207	0.8
	2−2	9120.3246	−0.9		4−3	17443.5019	0.5
	2−1	9120.3589	−0.7	514−505	6−6	3676.9570	0.0
	1−1	9121.3264	−1.6		5−5	3676.3071	0.0
	1−0	9121.2417	−1.1		4−4	3677.0969	0.5
211−202	3−3	3613.2293	0.8	515−505	6−6	3516.9057	0.2
	2−2	3612.6844	0.7		5−5	3517.4332	−0.1
	1−1	3613.5980	−0.2		4−4	3516.7739	0.3
212−202	3−3	3581.0180	0.7	524−514	6−6	10709.2047	1.2
	2−2	3581.5956	0.4		5−5	10709.8594	1.3
	1−1	3580.6307	0.3		4−4	10709.0668	1.0
	2−1	3581.5418	0.5	523−514	6−6	10710.0346	1.1
	3−2	3581.0535	1.5		5−5	10710.6758	1.2
	1−2	3580.6841	−0.2		4−4	10709.8995	0.5
221−211	3−3	10775.5254	−0.2	616−523	6−5	5616.7917	−0.1
	2−2	10776.1405	−1.1	616−524	6−5	5617.6081	−0.2
	1−1	10775.1155	−1.4	615−524	7−6	5840.9133	−0.2
	1−2	10776.0833	−2.0		6−5	5840.2494	0.2
	2−1	10775.1739	0.6		5−4	5841.0267	−0.7
220−211	3−3	10775.5495	−0.2	615−523	7−6	5840.0834	−0.1
	2−2	10776.1629	−1.3		6−5	5839.4322	−0.5
	1−1	10775.1406	−1.6		5−4	5840.1936	−0.7
	2−1	10775.1957	−0.1	616−606	7−7	3485.1782	−0.9
303−212	4−3	4680.0974	−1.1		6−6	3485.8200	−0.3
	3−2	4679.5209	−1.1		5−5	3485.0666	−1.0
	2−1	4680.4762	−1.4	615−606	7−7	3709.1275	−0.5
313−202	4−3	11826.0178	0.7		6−6	3708.4601	−1.1
	3−3	11826.5690	−0.4		5−5	3709.2419	−0.6
	2−2	11825.8290	−0.7	625−615	7−7	10676.0852	−0.6
	2−1	11825.7752	−0.5		6−6	10676.7457	−0.7
321−212	4−3	19068.2387	0.0		5−5	10675.9708	−1.0
	3−2	19067.6909	−0.4	624−615	7−7	10677.7439	−0.8
	2−1	19068.6073	−0.9		6−6	10678.3853	−0.4
322−212	4−3	19068.1192	−0.1		5−5	10677.6333	−0.8
	3−2	19067.5751	−1.1	616−505	5−4	20238.6177	0.4
	2−1	19068.4862	−1.0		7−6	20238.4128	0.9
313−303	4−4	3629.0917	0.5		6−5	20237.3618	0.9
	3−3	3628.4899	0.4	707−616	8−7	15783.3540	2.3
	2−2	3629.3218	0.2		7−6	15782.7189	1.9
313−303	4−4	3564.9020	0.7		6−5	15783.4632	1.9
	3−3	3565.5145	0.5	717−606	8−7	22716.9636	−1.0
	2−2	3564.6682	0.5		7−6	22717.6120	−1.5
322−312	4−4	10759.0496	0.3		6−5	22716.8660	−2.1
	3−3	10759.6796	−0.3	716−606	8−7	23015.4595	−1.1
	2−2	10758.8093	0.3		7−6	23014.7861	−1.4
322−312	4−4	10758.9304	0.5		6−5	23015.5577	−0.4
	3−3	10759.5644	−0.4	808−717	9−8	18569.5729	1.8
	2−2	10758.6881	0.1		8−7	18568.9380	1.5
404−312	5−4	7384.9885	−0.3		7−6	18569.6651	0.7
	3−2	7384.7536	−0.5	909−818	10−9	21359.4158	−1.5
404−313	5−4	7449.1781	−0.3		9−8	21358.7833	−1.7
	3−2	7449.4070	−1.0		9−8	21358.7833	−1.7
	3−2	7449.4070	−1.0		8−7	21359.4968	−1.4
413−303	5−4	14664.3890	0.8				
	4−3	14663.7604	0.4				
	3−2	14664.5558	0.3				

TABLE 1 (Continued)

$J''K_a''K_c''-J'K_a'K_c'$	F″−F′	obs (MHz)	obs − calc (kHz)	$J''K_a''K_c''-J'K_a'K_c'$	F″−F′	obs (MHz)	obs − calc (kHz)
Additional a-Type Transitions							
212−111	3−2	5496.8819	−0.3	312−211	2−1	8276.8306	−0.8
	2−1	5496.9891	−0.5	413−312	3−2	11035.2341	0.2
	1−0	5497.8425	−1.1		4−3	11035.2701	−0.4
211−110	1−0	5517.3584	−1.2		5−4	11035.2976	0.3
	2−1	5518.0717	−0.2	505−404	4−3	13766.4046	−0.5
	3−2	5518.2489	−0.4		6−5	13766.4102	0.8
322−221	3−2	8260.3466	0.5		5−4	13766.4142	1.4
	4−3	8260.3838	1.3	606−505	7−6	16517.9477	1.7
	2−1	8260.4036	1.1		5−4	16517.9477	0.6

TABLE 2: Rotational, Centrifugal Distortion (van Eijck), and Quadrupole Coupling Constants of Isoxazole−Argon, I^r Representation

$A = 4974.2534(2)$ MHz
$B = 1382.291788(24)$ MHz
$C = 1371.647236(36)$ MHz
$D_J' = 5.62421(30)$ kHz
$D_{JK}' = 34.8064(34)$ kHz
$D_K' = -27.8794(256)$ kHz
$\delta_J' = -0.01048(24)$ kHz
$R_6' = -0.00040(18)$ kHz
$\chi_{aa} = -0.11310(48)$ MHz
$\chi_{min}{}^a = 3.76962(750)$ MHz
$\chi_{bc} = \pm 4.8954(22)$ MHz

Calculated

$\chi_{bb} = 1.94136(87)$ MHz
$\chi_{cc} = -1.82826(45)$ MHz

174 components fitted, standard deviation = 0.92 kHz
highest correlation coefficient (C, D_J') = 0.86

[a] $\chi_{min} = \chi_{bb} - \chi_{cc}$.

TABLE 3: Remeasured Transitions of Isoxazole

$J''K_a''K_c''-J'K_a'K_c'$	F″−F′	obs (MHz)	diff[a] (kHz)
101−000	0−1	14411.7378	
	2−1	14412.0059	−4.9
	1−1	14412.1478	−2.2
111−000	1−1	14623.1151	
	2−1	14623.2633	−3.0
	0−1	14623.5220	2.6
110−111	0−0	4737.8748	
	2−2	4738.1389	1.2
	1−1	4738.2866	−1.0
110−101	1−1	4949.2543	
	2−2	4949.3963	2.2
	0−0	4949.6589	2.0
202−111	2−1	24079.0904	
	3−2	24078.9382	0.6
	1−0	24078.6692	1.9
212−111	2−1	24085.9871	
	3−2	24085.8430	−0.4
	1−0	24085.5773	1.5
202−101	1−0	24290.4540	
	3−2	24290.1953	−1.3
	2−1	24290.0575	−1.6
212−101	1−0	24297.3626	
	3−2	24297.1009	−2.1
	2−1	24296.9544	−0.8
221−212	1−1	14214.3157	
	3−3	14214.4129	−2.7
	2−2	14214.5724	0.1
211−202	1−1	14221.2252	
	3−3	14221.3180	−2.2
	2−2	14221.4686	2.5
330−321	2−2	5507.5343	
	4−4	5507.4696	−1.2
	3−3	5507.2839	−0.2
330−331	2−2	4240.2121	
	4−4	4240.2687	−1.9
	3−3	4240.4204	−0.7

[a] Diff: difference between observed and calculated hfs splitting between the first frequency of the transition and the frequency in the line referred to.

splittings of the two $J = 1-0$ transitions. This provides a seldom example for the determination of an off-diagonal element of the quadrupole coupling tensor of nitrogen without isotopic substitution. The remeasured transitions are given in Table 3, elements of the quadrupole coupling tensor and the highest correlation coefficient in Table 4.

2.2. Discussion. We used the rotational constants of isoxazole−argon to determine the position of the argon atom. In order to obtain the geometry of isoxazole−argon we assumed that the geometry of the isoxazole ring would remain unchanged upon complexation. Accordingly, we used the "best geometry" given by Stiefvater and co-workers for isoxazole.[2] Since it was possible to measure only the main isotopomer we could only determine the values of the coordinates of the argon atom but not the direction as explained previously in connection with oxazole−argon.[14] Isoxazole is a planar molecule. Other elements of symmetry are missing. The geometries with the argon atom above and below the ring plane form pairs of enantiomers which we cannot distinguish experimentally. In Figure 3 the two enantiomers of geometry **2** are given as an example. We obtained four possible r_0 geometries for the pairs of enantiomers given in Table 5 by a least-squares fit. All geometries reproduce the rotational constants. The four positions of the argon atom projected onto the ring plane of isoxazole are shown in Figure 4. In each of the four geometries, the argon atom is located 3.45 Å above or below the ring plane. As in the case of oxazole−argon,[14] we calculated a geometry by using the procedure of obtaining a r_s geometry for rigid molecules, which is based on differences in moments of inertia. We took the complex isotopomers with argon mass 40 and mass 0 where the latter corresponds to isoxazole itself. Although vibrational effects on the moments of inertia do not cancel each other out as in the case of rigid molecules, the term "r_s" is used to indicate the procedure of calculation. The geometries obtained in this way are in reasonable agreement with the r_0 geometries based on the moments of inertia of the complex. The differences in the r_s and r_0 coordinates of Ar reflect the large-amplitude motions of the complex partners with regard to each other. Due to experimental limitations an adequate account of the large amplitude motions was not possible.

The r_s type R value is 3.436 Å. Figure 4 also shows the projected positions of the argon atom onto the ring plane of isoxazole indicated by circles. Coordinates of the r_s geometry are given in Table 6. Comparison with the four possible geometries of oxazole−argon[14] reveals that in isoxazole−argon the argon atom is moved still further away from a location above/below the center of mass of the ring. This effect could be due to increased charge polarization in the isoxazole ring due to the presence of two directly connected electronegative atoms, nitrogen and oxygen, which in oxazole are separated by one carbon atom.

TABLE 4: Quadrupole Coupling Constants[a] of Isoxazole in the III^r Representation

$\chi_{\min}$[b]	1.021(3) MHz
χ_{cc}	0.0022(10) MHz
χ_{ab}	±5.40(10) MHz[c]
χ_{ac}	0.00 MHz[d]
χ_{bc}	0.00 MHz[d]
	Calculated
χ_{aa}	0.509(2) MHz
χ_{bb}	−0.512(2) MHz

highest correlation coefficient ($\chi_{\min},\chi_{ab}$) = −0.79

[a] Rotational constants, see ref 2. [b] $\chi_{\min} = \chi_{aa} - \chi_{bb}$. [c] The sign was determined to be positive by ref 30. On the question of the sign of off-diagonal elements of the quadrupole coupling tensor; see ref 31. [d] Due to symmetry.

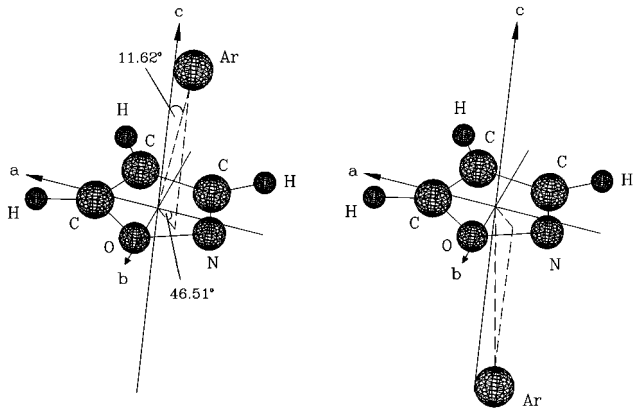

Figure 3. Enantiomer pair of isoxazole−argon corresponding to geometry **2**. The coordinate system is the principal axes system of isoxazole. The radii of the spheres correspond to the van der Waals radii of the atoms divided by 5. R_{exp} is the distance between Ar and ring plane. The line from argon to the center of mass of isoxazole encloses an angle of 11.62° with the *c*-axis while the projection of this line onto the molecular plane of isoxazole encloses an angle of 46.51° with the *a*-axis.

As in the case of oxazole−argon we tried to distinguish between the four different geometry pairs of isoxazole−argon by regarding the hyperfine structure. If the electronic surrounding of the nitrogen nucleus of isoxazole is assumed to remain nearly unchanged upon complexation, the differences in the quadrupole coupling tensor of isoxazole and isoxazole−argon should only be due to a rotation of the principal axis system. This method was successfully applied with oxazole−argon.[14] However, it failed for reasons unknown with isoxazole−argon. The calculated quadrupole coupling tensors for each geometry of isoxazole−argon are presented in Table 5 for the r_0 structures and in Table 6 for the r_s structures.

Because of this failure we were looking for another method to distinguish between the different geometries of isoxazole−argon. We found one in relating the line intensities of different transitions to different components of the dipole moment vector. The intensity of a transition, I, is defined as[20]

$$I = \int \alpha(\nu)\, d\nu \tag{1}$$

where ν denotes the frequency and α the absorption coefficient, which is proportional to the square of the dipole matrix element at given experimental conditions such as temperature and pressure:

$$\alpha(\nu) \approx |\langle m|\mu|n\rangle|^2 \tag{2}$$

In (2), m and n denote the initial and final state of a transition

TABLE 5: r_0 Geometries 1−4 of Isoxazole−Argon[a]

Geometry **1**

	a	*b*	*c*	χ
N(1)	−1.1069	0.3902	0.0000	
O(2)	0.0958	1.1047	0.0000	
C(3)	1.1173	0.2322	0.0000	
C(4)	0.6554	−1.0428	0.000	$\begin{pmatrix} 0.309 & \pm 0.454^b & \mp 1.174^b \\ & -4.536 & -2.927 \\ & & 4.227 \end{pmatrix}^c$
C(5)	−0.7589	−0.8721	0.0000	
H(3)	2.1033	0.6604	0.0000	
H(4)	1.2181	−1.9578	0.0000	
H(5)	−1.5336	−1.6210	0.0000	
Ar	0.4876	−0.5137	$\pm 3.4488^b$	

Geometry **2**

	a	*b*	*c*	χ
see geometry **1**				$\begin{pmatrix} -0.307 & \pm 0.218^b & \mp 1.241^b \\ & 5.009 & 2.046 \\ & & -4.703 \end{pmatrix}^c$
Ar	0.4875	0.5139	$\pm 3.4488^b$	

Geometry **3**

	a	*b*	*c*	χ
see geometry **1**				$\begin{pmatrix} -0.307 & \mp 0.218^b & \pm 1.241^b \\ & 5.009 & 2.046 \\ & & -4.703 \end{pmatrix}^c$
Ar	−0.4875	−0.5140	$\pm 3.4488^b$	

Geometry **4**

	a	*b*	*c*	χ
see geometry **1**				$\begin{pmatrix} 0.309 & \mp 0.4541b & \pm 1.174^b \\ & -4.536 & -2.927 \\ & & 4.227 \end{pmatrix}^c$
Ar	−0.4875	0.5138	$\pm 3.4488^b$	

[a] a, b, c: coordinates in the principal axes system of isoxazole. χ: calculated quadrupole coupling tensor derived from the quadrupole coupling tensor of isoxazole. [b] The calculated upper sign belongs to the geometry with the argon atom above the ring plane and the lower sign to the geometry with the argon atom below the ring plane. [c] The values should be compared with the experimentally derived values in Table 2.

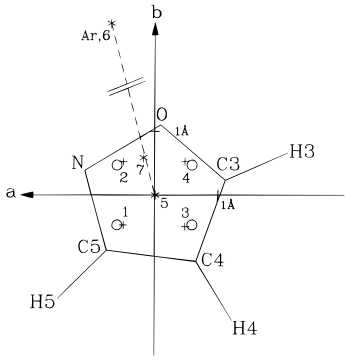

Figure 4. Possible geometries of isoxazole−argon. For geometries **1**, **2**, **3**, **4**, **5**, and **7**, the projection of the position of Ar onto the ring plane of isoxazole is indicated by crosses or stars. The coordinate system is the principal axes system of isoxazole. Numbering of the ring atoms is shown. r_s geometries **1**−**4** are indicated by circles and the corresponding r_0 geometries by crosses. For geometry **6**, the Ar−O distance has been reduced as indicated by the symbol ||.

and μ is the dipole moment. For a field-free rotor, the dipole matrix element can be written as

$$|\langle m|\mu|n\rangle|^2 = \lambda_g \mu_g^2 \tag{3}$$

λ_g denotes the line strength of a transition and is tabulated for various transitions;[21] μ_g is the specific component of the dipole moment vector, which induces the transition. Now it can be seen that with given experimental conditions the line intensity

TABLE 6: r_s Geometries 1−4 of Isoxazole−Argon

Geometry **1**

	a	b	c	χ		
	see Table 5			0.351	∓0.094[b]	∓1.334[b] [b]
					−5.200	1.519
Ar	0.593	−0.471	±3.436[b]			4.848

Geometry **2**

	a	b	c	χ		
	see Table 5			−0.332	∓0.166[b]	∓1.333[b] [b]
					5.384	0.551
Ar	0.593	0.471	±3.436[b]		−5.053	

Geometry **3**

	a	b	c	χ		
	see Table 5			−0.332	±0.166[b]	±1.333[b] [b]
					5.384	0.551
Ar	−0.593	−0.471	±3.436[b]			−5.053

Geometry **4**

	a	b	c	χ		
	see Table 5			0.351	±0.094	±1.334[b] [b]
					−5.200	1.519
Ar	−0.593	0.471	±3.436[b]			4.848

[a] a, b, c, and χ, see Table 5. [b] See Table 5.

I is proportional to μ_g^2 and the transition line strength:

$$I \approx \lambda_g \mu_g^2 \tag{4}$$

We have measured Q-branches in the scanning mode which causes equal experimental conditions for the transitions. One Q-branch can be seen in Figure 5. In that spectrum, *b*- and *c*-type transitions are shown which have equal line strength for equal J quantum number.[21] So it is possible just to relate the height of each peak of a *b*-type transition to its *c*-type counterpart in order to get information about the relative magnitude of μ_b and μ_c. It can be seen that μ_c has to be larger than μ_b. We assumed that the dipole moment vector of isoxazole would not change upon complexation with argon despite the existence of an induced dipole moment. The latter dipole moment can be estimated to be of the order of 0.12 D because of dipole moment measurements of benzene−argon by Brupbacher and Bauder.[8] Accordingly, 0.12 D is the magnitude of uncertainty in calculating a dipole moment vector for each geometry of isoxazole−argon by rotating the known dipole moment vector of isoxazole into the four principal axes systems:

$$\mu_{Is-Ar} = \mathbf{D}\mu_{Is} \tag{5}$$

where **D** is the rotation matrix. The results are given in Table 7. One can see that only for geometries **2** and **3** the magnitude of the calculated μ_c is larger than that of μ_b. Furthermore, with geometry **2** and **3** μ_a should be large enough to enable us to measure also *a*-type transitions. Indeed, with new measurements we found *a*-type transitions in good intensity. The measured *a*-type transitions are given in Table 1. Because of these results, we favor geometry **2** or **3** to represent the most stable complex geometry. With the method discussed above, a selection of one of these geometries as the most stable geometry is not possible. Since investigations of the furan−argon,[12] pyrrole−argon,[13] or oxazole−argon van der Waals complex[14] showed that the argon atom is shifted toward the electronegative part of the ring, it seems reasonable to favor geometry **2**. In this geometry, the argon atom is shifted toward the two electronegative atoms oxygen and nitrogen of isoxazole while in geometry **3** the argon atom is oriented in the direction the positively charged atom C4. This hypothesis is tested in the following sections with the help of ab initio calculations and the model for van der Waals complexes developed recently.[14]

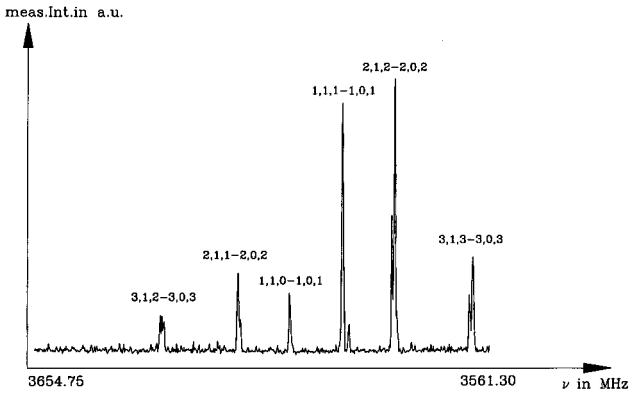

Figure 5. Automatically scanned amplitude spectrum of a Q-branch of isoxazole−argon; spectrum recorded with 128 cycles with 1K Fourier transformation and a step width of 0.25 MHz. The three μ_c-type transitions in the upper frequency region are more intense.

TABLE 7: Calculated Dipole Moments of r_0 Geometries 1−4 of Isoxazole−Argon[a]

	calculated dipole moment
geometry **1**	±0.040[b] [c] −2.787 −0.800
geometry **2**	∓0.691[b] [c] 0.593 −2.755
geometry **3**	±0.691[b] [c] 0.593 −2.755
geometry **4**	∓0.040[b] [c] −2.787 −0.800

[a] The coordinate systems used are the principal axes systems of the corresponding complexes. [b] The upper sign is due to the geometry with the argon atom above the ring plane and the lower to the geometry with the argon atom below the ring plane. The sign is without influence on our investigation. [c] We know the relative sign of μ_a and μ_b of isoxazole from rotating the dipole moment of isoxazole from its principal axes system into the principal axes system of 4-D-isoxazole. The dipole moment of 4-D-isoxazole was measured by ref 30. A comparison of the measured values with the calculated values shows that either $\mu_a > 0$ and $\mu_b < 0$ or $\mu_a < 0$ and $\mu_b > 0$. We arbitrarily chose $\mu_a > 0$, $\mu_b < 0$.

3. Ab Initio Calculations

Theoretical calculations of van der Waals complexes require a basis set that is flexible enough to reproduce the different contributions to the interaction energy but is not too expensive for high-level correlation corrected calculations. As discussed in the case of the oxazole−argon complex,[14] an appropriate choice for Ar is the (14s10p2d1f)[7s4p2d1f] basis set of Chalasinski, Funk, and Simons,[22] being designed to calculate polarizabilities and dispersion energies. This basis keeps the two most diffuse sp functions of the (14s10p) set uncontracted while the exponents of added d- and f-type polarization functions are optimized to accurately describe the dispersion energy of Ar_2. Although the resulting DZ+(2d1f) basis set is of moderate size (36 basis functions for Ar), it reproduces the Ar polarizability at the MP2 level with an error of just 4%.[14]

As in the case of the oxazole−argon complex, we use for the isoxazole ring Spackman's 6-31G(+sd,+sp) basis set, which is obtained from Pople's 6-31G basis by adding diffuse s- and

TABLE 8: Comparison of Experimental and Theoretical Geometries of Isoxazole[a]

parameter	exp[b]	HF/6-31G-(+sd,+sp)	MP2/6-31G-(+sd,+sp)	MP2/6-31G(d)
R(N−C5)	1.309	1.294	1.354	1.328
R(C4−C5)	1.425	1.436	1.443	1.414
R(C4−C3)	1.356	1.345	1.384	1.364
R(C3−O)	1.343	1.350	1.406	1.353
R(N−O)	1.399	1.412	1.486	1.391
R(C3−H3)	1.075	1.069	1.089	1.076
R(C4−H4)	1.075	1.068	1.090	1.075
R(C5−H5)	1.077	1.071	1.093	1.078
α(N−C5−C4)	112.2	112.3	113.2	112.2
α(C5−C4−C3)	103.0	103.7	105.0	103.5
α(C4−C3−O)	110.6	110.0	110.0	110.0
α(C3−O−N)	108.7	108.9	107.8	109.2
α(O−N−C5)	105.3	105.1	104.0	105.1
α(C4−C3−H3)	133.4	133.4	135.1	134.3
α(C5−C4−H4)	128.5	127.9	127.8	128.6
α(N−C5−H5)	118.7	119.2	118.0	118.5

[a] Bond lengths R in Å, bond angles α in deg. For numbering of atoms see Figure 4. [b] r_s geometry from refs 2 and 3.

d-functions to the heavy atom basis sets and diffuse s and p functions to the H basis set.[23] The exponent of the diffuse s function for the heavy atoms is set equal to $^1/_4$ of the value of the outermost sp functions of the 6-31G basis while the exponent of the diffuse s function for H is set to 0.040. The exponents of the polarization functions are optimized so that the mean polarizability of AH_n hydrides adopts a maximum value. With this basis set, HF and MP2 polarizabilities are obtained with an error of less than 15 and 5%, respectively.[23]

An important prerequisite for a reliable description of van der Waals complexes is the correction for basis set superposition errors (BSSEs); i.e., calculations have to be basis set consistent.[24] In this work, the counterpoise (CP) procedure of Boys and Bernardi[25] was applied, according to which both complex and monomers are calculated with the dimer-centered basis set (DCBS).[24] In particular for moderately seized basis sets, CP corrections are essential for supermolecular perturbation theory. Therefore, all calculations including energy, geometry, and other property calculations of the isoxazole−argon complex were carried out with the CP method using the DCBS. In the case of the isoxazole−argon complex, BSSE corrections lead to changes in the binding energy by 100−150% and changes in the geometry by 50%.

The geometry of isoxazole was optimized at the HF and MP2 level of theory using the 6-31G(+sd,+sp) basis set. HF and MP2 geometrical parameters obtained in these calculations (Table 8) differ considerably where only the HF geometry is close to the r_s geometry determined by MW spectroscopy.[2,3] In previous work, we have shown that this is due to the relative large number of diffuse functions contained in the Spackman basis. At the MP2 level, this leads to an expansion of the electron density distribution and, as a consequence, to significant bond lengthening. By deleting the diffuse functions and determining the equilibrium geometry at the MP2/6-31G(d) level of theory (see Table 8), bond lengths and angles are obtained that are in reasonable agreement with experimental r_s values. Since it is not reasonable to calculate the equilibrium geometry of isoxazole with one basis and that of the complex with another basis, the geometry of isoxazole was frozen at the experimental r_s geometry and used in all complex calculations. This is a reasonable approach since test calculations revealed that the isoxazole geometry is hardly changed by complex formation.

Because of the necessary BSSE corrections, the optimization of the Ar position was done numerically by establishing a grid of energy points that correspond to specific positions of the Ar atom above the plane of the isoxazole ring. These positions include (among other) the four positions of Ar belonging to geometries **1**−**4** and a position of Ar above the center of mass of the five-membered ring (geometry **5**, see Figure 4). For each position, the distance R from the ring plane was optimized explicitly considering BSSEs by the CP procedure. The exact position was then determined by fitting calculated energy points with optimized R values to a two-dimensional function and calculating the minimum of this function. This led to the ab initio equilibrium position of Ar (geometry **7**, see Figure 4).

Initial calculations were carried out with the HF method since qualitative descriptions of van der Waals complexes that are stabilized by multipole interactions can already be obtained at this level of theory. However, a reasonable description of van der Waals complexes requires a correlation corrected method.[6] For this purpose, we applied MP2, MP3, and MP4 perturbation theory[15] where in the latter case all single (S), double (D), and quadruple (Q) excitations were included (MP4(SDQ)). In addition, full MP4 calculations including all triple (T) excitations (MP4(SDQTQ)) were performed to test the importance of three-electron correlation effects. The MP/DZ+P calculations carried out in this work should lead to reasonable complex geometries; however, it is appropriate to note that highly accurate complex stabilization energies require much larger basis sets.[6a] All calculations were carried out with the COLOGNE94[26,27] and ACES II[28] ab initio packages.

4. Results and Discussion

In Table 9, optimized R values for geometries **1**−**7** (Figure 4) are summarized together with absolute and relative energies obtained at various levels of theory.

At the HF level, a stable isoxazole−argon complex was not found irrespective of the position of the Ar atom either above or in the plane of the isoxazole ring. During the HF geometry optimization the distance between Ar and isoxazole increases to large R values while the binding energy decreases from positive values toward a zero value. Obviously, exchange repulsion effects are larger than stabilizing inductive effects while dispersion effects are not covered by the HF approach.

At the MP2 level, the Ar atom is bound to the ring by about 270−296 cm^{-1} (800−850 cal/mol) no matter whether geometry **1**, **2**, **3**, or **4** is adopted (Table 9). The optimized R values vary from 3.67 Å (position **1**) to 3.58 Å (position **2**), i.e., in all cases the calculated distance between Ar and the ring plane is larger than the experimental r_s value of 3.44 Å, which could have to do with the use of the Spackman basis as discussed in connection with the isoxazole geometry. Comparing the binding energies of **1**, **2**, **3**, and **4**, it turns out that **2**, which corresponds to an Ar position near the middle of the NO bond, represents the most stable complex configuration with a binding energy of 296 cm^{-1} (850 cal/mol) and a R value 0.14 Å larger than the experimental r_s value. Differences in the energies between geometries **1**−**4** range from 15 to 64 cm^{-1} (42 to 182 cal/mol). If one places the Ar atom exactly above the ring center (geometry **5**), the difference in energies of **2** and **5** reduces to just 7 cm^{-1} (20 cal/mol), indicating the flatness of the potential energy surface (PES) with regard to horizontal displacements of Ar.

Exploration of the isoxazole−argon PES in the region of geometries **1**−**5** reveals that there is only one optimal position of the Ar atom above the isoxazole ring plane, namely the position associated with geometry **7**, which is between **2** and **4** (but closer to **2**; see Figure 4). Geometries **1**−**5** represent transient points on the isoxazole−argon PES that have no particular importance for the isoxazole−argon complex apart from the fact that they characterize the flatness of the PES in

TABLE 9: Stabilization Energies ΔE of Isoxazole−Argon for Geometries 1−7 Calculated at Experimental and Optimized Distances R[a]

			$R_{exp} = 3.449$						
method	geometry	Ar closest to	ΔE	$\Delta\Delta E$	R_{opt}	a	b	ΔE	$\Delta\Delta E$
MP2	**1**	C5	−215	79	3.669	0.487	−0.514	−270	26
	2	N, O	−294	0	3.576	0.487	0.514	−296	0
	3	C4	−175	119	3.693	−0.487	−0.514	−232	64
	4	C3, O	−274	20	3.606	−0.487	0.514	−281	15
	5	center	−279	15	3.623	0.	0.	−289	7
	6	N, O (in plane)			4.189	0.643	3.440	−180	116
	7	N, O	−305	−11	3.527	0.162	0.638	−308	−12
MP3	**7**	N, O	−195		3.683	0.162	0.638	−215	
MP4(SDQ)	**7**	N, O	−202		3.657	0.162	0.638	−216	
MP4(SDTQ)	**7**	N, O	−281		3.547	0.162	0.638	−283	

[a] Relative energies ΔE in cm^{-1}, R and coordinates a and b in Å (see Figure 4). MP2, MP3, MP4(SDQ), and MP4(SDTQ) energies of geometry **7** for R_{exp}: −771.998 30, −772.011 46, −772.028 17, −772.060 34, and for R_{opt} −771.998 01, −772.010 83, −772.027 45, −772.059 94 hartrees.

the vicinity of minimum **7**. The MP2 complex binding energy for **7** is 308 cm^{-1} (880 cal/mol) and the distance R is 3.53 Å (Table 9), which is smaller than the corresponding values for geometries **1**−**5**, but still 0.09 Å larger than the r_s value of 3.44 Å.

At MP3 and MP4(SDQ), distance R of minimum **7** increases to 3.68 and 3.66 Å, respectively. The inclusion of T excitations at the MP4 level reduces R to 3.55 Å, which is close to the MP2 value (Table 9). The complex binding energies show the reverse trend; i.e., MP2 and MP4(SDTQ) binding energies are of similar magnitude while MP3 and MP4(SDQ) lead to smaller values. The similarity of MP2 and MP4 results suggests that supermolecular perturbation theory at the MP2 level is already sufficient to approximate the more accurate MP4(SDTQ) description of the isoxazole−argon complex.

If Ar is placed in the plane of the isoxazole ring opposite to the middle of the ON bond (geometry **6**), a relatively large distance of 4.19 Å is calculated. The complex stability decreases to 180 cm^{-1} (515 cal/mol), which is typical of positions in the ring plane opposite to one of the ring atoms or ring bonds. Positions above and below the ring plane are energetically favored compared to positions in the ring plane (see below). Since **6** is about 130 cm^{-1} (370 cal/mol) higher in energy than the equilibrium form **7**, it is unlikely that **6** or related forms can be detected in molecular beam experiments. Of the possible geometries **1**−**4** suggested by experiment, only geometry **2**, which is closest to the MP2 minimum geometry **7**, is likely to represent the most stable geometry of the experiment. Both **7** and **2** position the Ar atom closer to the most electronegative atoms of the ring, oxygen and nitrogen, which is in line with our prediction based on a model description of Ar van der Waals complexes.

The fact that the Ar atom preferentially approaches the most electronegative ring atom, is also reflected by calculated dipole and quadrupole moments for isoxazole and its Ar complex (see Table 10). Interaction of argon with the ring leads to a small induced dipole moment along the c axis. The μ_c component calculated at the MP2 level is generally rather small, but, however, adopts its largest value for geometries **2** and **7** (−0.05 and −0.04 D), which confirms that in these geometries induction forces are strongest. We note that the magnitude of calculated μ_c component and total dipole moment is in line with the assumption made in section 2, namely that the total dipole moment of isoxazole−argon can be represented by that of isoxazole for which $\mu_c = 0$ by symmetry (Table 10).

Negative quadrupole moment components reflect the expansion of electron density into space. In case of geometries **2** and **7**, the largest Q_{cc} values are found (−3.71 and −3.62 10^{-26} esu cm^2), suggesting relatively strong polarization interactions between Ar and ring for these geometries. With regard to isoxazole, there is a small increase of Q_{cc} in magnitude, again indicating the polarization of the electrons of isoxazole and Ar atom in the direction of the c axis.

TABLE 10: Polarizability α, Dipole Moment μ, and Quadrupole Moments Q of Isoxazole and Its Ar Complex Calculated for Different Geometries and Compared with Available Experimental Data[a]

		exptl geometry		opt geometry	
property	exptl values[b]	HF	MP2	HF	MP2
		A. Isoxazole			
α		47.08	50.06	44.35	48.89
μ_a	−1.98	−2.37	−2.15	−2.15	−1.72
μ_b	−2.12	−2.88	−2.34	−3.06	−2.81
μ_c		0.00_1	0.00_1	0.00_1	0.00_1
μ_{total}	2.9	3.73	3.18	3.74	3.29
Q_{aa}	0.1(11)	2.67	1.93	3.45	3.88
Q_{bb}	3.0(13)	1.14	1.24	0.32	−0.13
Q_{cc}	−3.1(16)	−3.81	−3.17	−3.78	−3.75
Q_{ab}		−5.41	−4.57	−5.32	−4.20
Q_{ac}		−0.01	−0.01	−0.01	0.01
Q_{bc}		+0.01	+0.01	+0.01	−0.01

	MP2 calculations				
	1	**2**	**3**	**4**	**7**
	B. Isoxazole−Argon				
μ_x[c]	−2.12	−2.11	−2.11	−2.11	−2.11
μ_y	−2.29	−2.31	−2.31	−2.31	−2.31
μ_z	−0.01	−0.05	0.01	0.01	−0.04
μ_{total}	3.12	3.13	3.13	3.13	3.13
Q_{xx}	2.13	2.21	2.03	2.06	2.14
Q_{yy}	1.33	1.50	1.33	1.43	1.48
Q_{zz}	−3.47	−3.71	−3.36	−3.46	−3.62
Q_{xy}	−4.54	−4.49	−4.59	−4.53	−4.51
Q_{xz}	0.12	0.17	0.13	0.22	0.21
Q_{yz}	0.20	0.12	0.12	0.08	0.10

[a] Polarizability in bohr^3, dipole moment in D, quadrupole moment in 10^{-26} esu cm^2. The coordinate system used for both parent molecule and complex is the principal axes system of isoxazole. Values for isoxazole are BSSE corrected, which in the case of dipole moment and quadrupole moment leads to small c components. For complex geometries **1**−**4**, the experimental distance R_{exp} = 3.449 Å and for geometry **7** the calculated distance R_{opt} = 3.527 Å is used. [b] Dipole moment from ref 3, quadrupole moment from ref 2. [c] x corresponds to the a-principal axis, y to the b-principal axis, and z to the c-principal axis of isoxazole.

In order to clarify which electronic forces lead to a larger stability of geometries **2** and **7**, we pursue the strategy developed for the investigation of the oxazole−argon complex, which has turned out to be rather useful for analyzing argon van der Waals complexes in general.[14] This work has shown that the complex stability is mainly due to dispersion forces while geometry and

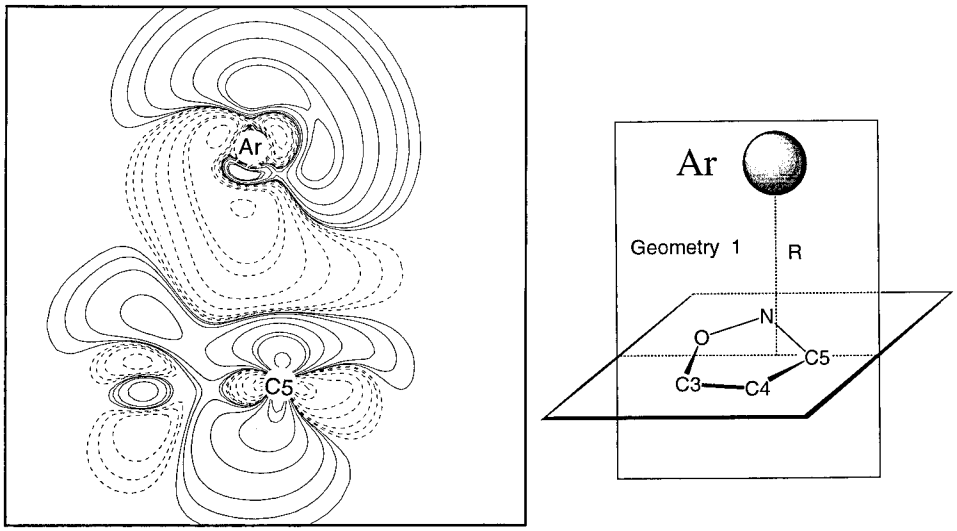

Figure 6. Contour line diagram of the MP2 difference electron density distribution of isoxazole−argon (geometry **1**), $\Delta\rho(\mathbf{r}) = [\rho(\text{isoxazole−argon}] - \rho(\text{isoxazole})^{\text{DCBS}} - \rho(\text{argon})^{\text{DCBS}}]$ using the 6-31G(+sd,+sp) basis for isoxazole and the [7s4p2d1f] basis for argon. The reference plane contains Ar and C5 as is schematically indicated in the figure. Contour lines range from 2×10^{-6} to 2×10^{-1} [e/bohr^3]. Solid lines correspond to an increase of electron density upon complex formation and dashed lines to a decrease.

electron density distribution of the complex are a result of exchange repulsion forces.[14] The argon atom has to approach its complex partner as close as possible to benefit from large stabilizing dispersion forces. However, exchange repulsion forces, which envelope isoxazole like a cloud, prevent Ar from coming too close to the ring. The two opposing forces direct Ar to a position which keeps exchange repulsion as small as possible but maximizes stabilizing dispersion and induction forces. In this way, exchange repulsion determines geometry and electron density distribution of the complex. Accordingly, an investigation of the electron density of the complex should reveal those positions in the vicinity of the isoxazole molecule where exchange repulsion is small. For the purpose of detecting these locations, we analyze the difference electron density $\Delta\rho(\mathbf{r})$

$$\Delta\rho(\mathbf{r}) = \rho(\mathbf{r})\text{complex} - [\rho(\mathbf{r})\text{isoxazole}^{\text{DCBS}} + \rho(\mathbf{r})\text{Ar}^{\text{DCBS}}] \tag{6}$$

which is defined as the difference between the electron density of the complex and the electron densities of the noninteracting complex partners kept at the positions they adopt in the complex. In eq 6, the abbreviation DCBS indicates that the electron densities of isoxazole and Ar are corrected for BSSE errors using the CP method.

In Figures 6, 7, 8, and 9, contour line diagrams of the MP2 difference electron density distribution of the isoxazole−argon complex are shown with regard to reference planes that are perpendicular to the plane of the isoxazole ring and that contain both the Ar nucleus and the nucleus of that atom which is next to the Ar atom, i.e., reference planes for geometries **1**−**4** contain beside the Ar nucleus also that for C5 (Figure 6), O (Figure 7a), N (Figure 7b), C4 (Figure 8), and C3 (Figure 9). In this way, the difference density plots in Figures 6−9 provide information about important electronic structure changes upon complexation.

All diagrams reveal a regular pattern of regions with increase (solid contour lines) and decrease (dashed contour lines) of electron density as a result of complex formation. Electron density is pushed out of the intermolecular region toward the back of the Ar atom. Similarly, the π-electron density of the isoxazole ring is pressed on to the ring atoms and through the center of the isoxazole ring so that a buildup of electron density can also be found on the back of the ring. In particular, there is a pronounced buildup of negative charge in front of that atom that is next to Ar and it is this accumulation of electron density that stops Ar from approaching the ring as close as possible in order to increase stabilizing dispersion interactions. In other words, the regions of charge buildup above the ring atoms provide a qualitative description of the regions with increasingly large exchange repulsion effects that hinder any closer approach of the two complex partners.

In the case of a carbon atom (geometries **1**, **3**, and **4**, Figures 6, 8, and 9), exchange repulsion starts "early" because of a somewhat more diffuse charge buildup above the carbon atoms C5, C4, and C3. In the case of the nitrogen atom (geometry **2**, Figure 7b), the Ar atom can approach the ring somewhat more because π-density is more contracted toward the more electronegative N atom thus reflecting the fact that exchange repulsion forces are smaller in this region than in the region above the C atoms. There is even further contraction of the region of large exchange repulsion above the O atom as is reflected by the stronger contraction of the charge buildup at this atom (geometry **2**, Figure 7a). There is a depression ("hole") in the enveloping sphere of large exchange repulsion above the O atom, which is a direct result of the large electronegativity of O that leads to a strong contraction of negative charge toward the O nucleus.

In comparison with the situation in the oxazole−argon complex, the hole in the exchange repulsion sphere of isoxazole is less developed at position **2** (or the minimum geometry **7**) than for the corresponding position found above the oxazole ring. This simply reflects the fact that for the latter ring, there is just one isolated depression region, namely that above the O atom, while in the isoxazole case the two depression regions above O and above N atom are adjoined thus giving the Ar atom the chance of a relatively close approach toward the ring while benefiting at the same time from the inductive effects of two rather than one electronegative atom. As a consequence, the optimal position of Ar is distinctively shifted from **5** (above center of mass) toward the ON bond of the ring.

We conclude that the position of the Ar atom above the ring is determined by reduced exchange repulsion above the O and N atom. Although these atoms possess more electrons than any

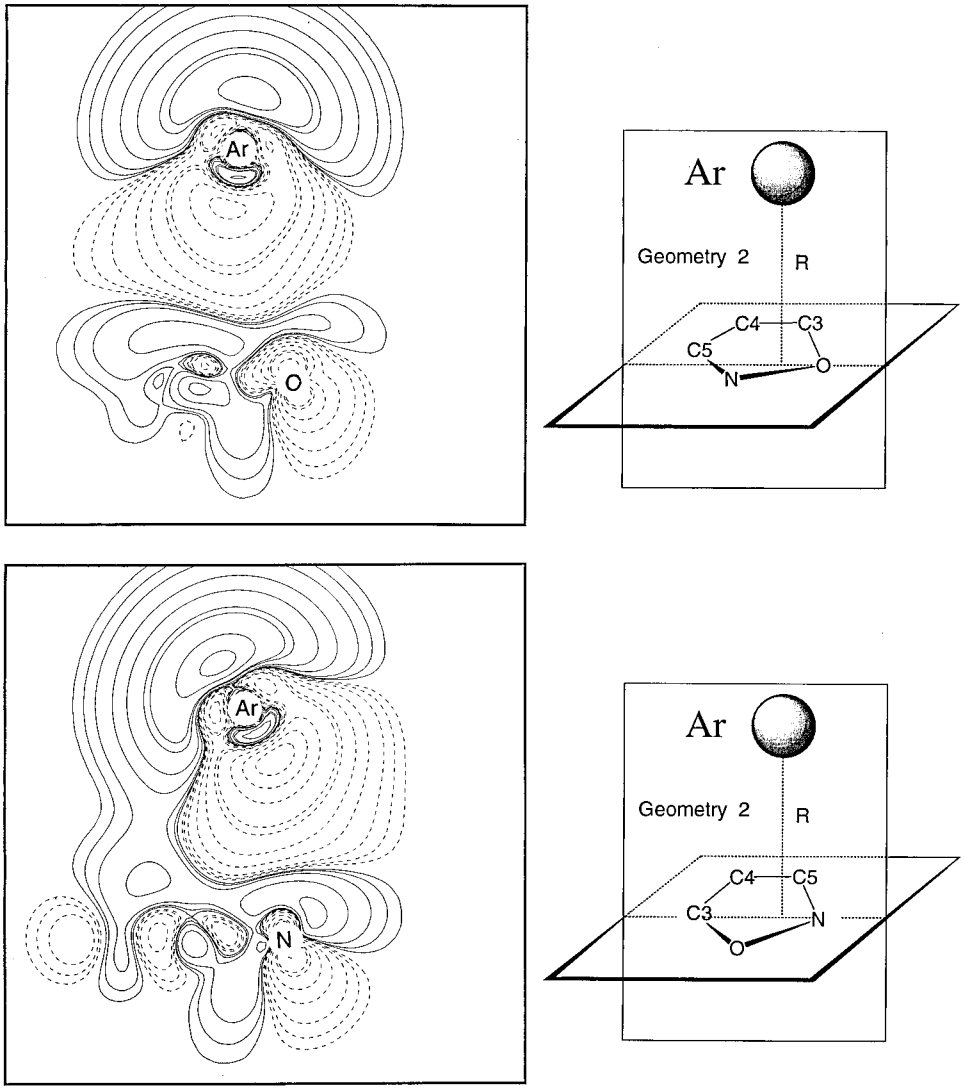

Figure 7. Contour line diagram of the MP2 difference electron density distribution of isoxazole−argon (geometry **2**), $\Delta\rho(\mathbf{r}) = [\rho(\text{isoxazole−argon}] - \rho(\text{isoxazole})^{DCBS} - \rho(\text{argon})^{DCBS}]$ using the 6-31G(+sd,+sp) basis for isoxazole and the [7s4p2d1f] basis for argon. The reference plane contains (a) Ar and O and (b) Ar and N as is schematically indicated in the figure. Contour lines range from 2×10^{-6} to 2×10^{-1} [e/bohr^3]. Solid lines correspond to an increase of electron density upon complex formation and dashed lines to a decrease.

other atom in the isoxazole ring, their negative charge is much more contracted and, as a consequence, their volumes are smaller.

As shown in our previous work on the oxazole−argon complex,[14] a similar explanation of the complex geometry is obtained by just analyzing the Laplace concentration of the electron density, $-\nabla^2\rho(\mathbf{r})$, of the partner molecule.[29] For isoxazole, $-\nabla^2\rho(\mathbf{r})$ exhibits holes in the π-space of O and the N atom, which suggest that an approaching electron-rich atom will prefer these sites because of low exchange repulsion. In this way, the analysis of the Laplace concentration provides a basis to qualitatively predict the most stable geometry of an Ar van der Waals complex.

Since exchange repulsion is in any case destabilizing, the complex has to be considered as being predominantly dispersion bound although exchange repulsion effects determine the position of the Ar atom. Any position of the Ar atom in the isoxazole plane leads to a less stable van der Waals complex although such an approach would lead to stronger stabilizing inductive effects. In the plane, exchange repulsion, in particular opposite to the in-plane lone pair electrons of O and N is rather strong as indicated by a somewhat more extended in-plane Laplace concentration compared to that perpendicular to the ring. In addition, the Ar atom feels the stabilizing dispersion interactions of just three atoms while above the ring dispersion interactions with five heavy atoms are possible.

5. Conclusions

The results of this work can be summarized in as follows.

1. The most stable geometry of the isoxazole−argon van der Waals complex is characterized by the Ar being located above (or below) the ring rather than in the ring plane, which is a result of intermolecular dispersion and exchange repulsion effects.

2. The measured ring−Ar distance R is 3.436 Å (r_s; r_0 3.449 Å), which is somewhat smaller than MP4(SDTQ)/6-31G-(+sd,+sp) and MP2/6-31G(+sd,+sp) distances of 3.527 and 3.547 Å (at equilibrium geometry **7**). While experimentally it is not possible to distinguish between an Ar position closer to either C4 (geometry **3**) or bond ON (geometry **2**), supermolecular MP perturbation theory at second, third, and fourth order clearly predicts a position closer to the NO bond ($a = 0.162$ Å, $b = 0.6376$ Å, $c = 3.527$ Å) to correspond to the global minimum of the isoxazole−argon complex (geometry **7**). Hence, of the four possible geometries suggested by experiment, geometry **2** (close to **7**) is the correct one.

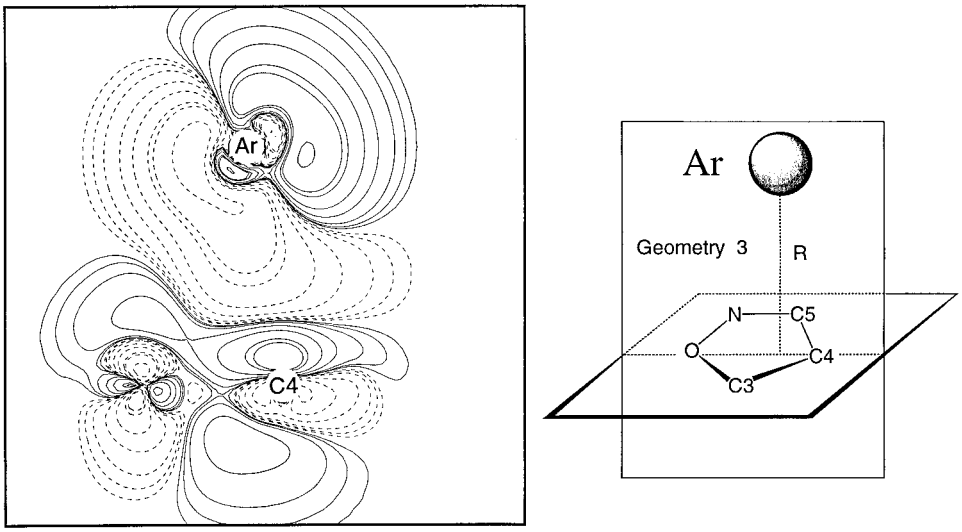

Figure 8. Contour line diagram of the MP2 difference electron density distribution of isoxazole−argon (geometry **3**), $\Delta\rho(\mathbf{r}) = [\rho(\text{isoxazole−argon}] - \rho(\text{isoxazole})^{DCBS} - \rho(\text{argon})^{DCBS}]$ using the 6-31G(+sd,+sp) basis for isoxazole and the [7s4p2d1f] basis for argon. The reference plane contains Ar and C4 as is schematically indicated in the figure. Contour lines range from 2×10^{-6} to 2×10^{-1} [e/bohr^3]. Solid lines correspond to an increase of electron density upon complex formation and dashed lines to a decrease.

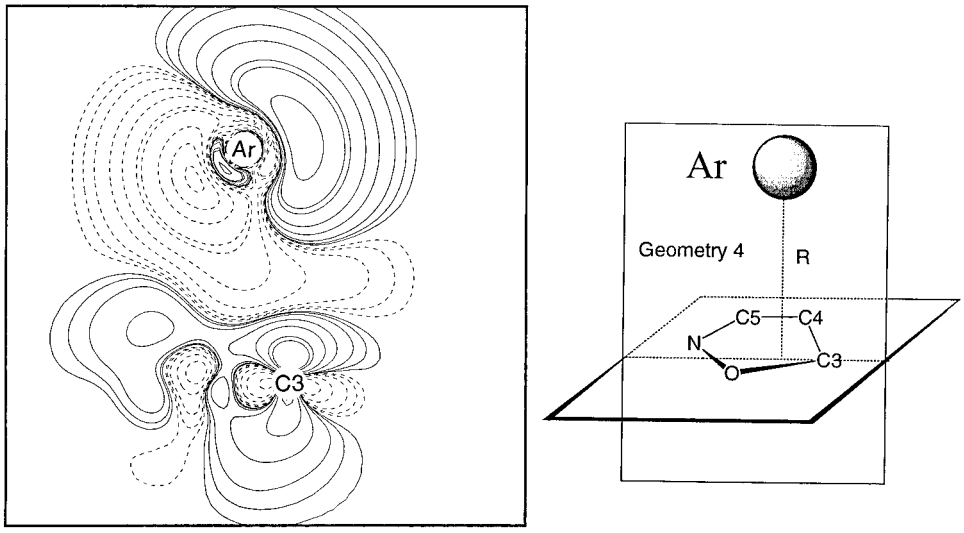

Figure 9. Contour line diagram of the MP2 difference electron density distribution of isoxazole−argon (geometry **4**), $\Delta\rho(\mathbf{r}) = [\rho(\text{isoxazole−argon}] - \rho(\text{isoxazole})^{DCBS} - \rho(\text{argon})^{DCBS}]$ using the 6-31G(+sd,+sp) basis for isoxazole and the [7s4p2d1f] basis for argon. The reference plane contains Ar and C3 as is schematically indicated in the figure. Contour lines range from 2×10^{-6} to 2×10^{-1} [e/bohr^3]. Solid lines correspond to an increase of electron density upon complex formation and dashed lines to a decrease.

3. The MP2 and MP4 complex stabilities are 308 and 283 cm^{-1} (880 and 990 cal/mol) at position **7** which compare well with the calculated binding energies for the oxazole−argon complex (MP2 316 cm^{-1} and MP4 304 cm^{-1} (904 and 870 cal/mol), ref 14).

4. As in the case of oxazole−argon, the isoxazole−argon complex is predominantly stabilized by dispersion interactions while inductive effects play a minor role, which is indicated by the fact that the complex is not bound at the HF level. Besides dispersion forces, exchange repulsion forces play an important role insofar as they determine the exact position of the Ar above the ring. Ar moves toward the atoms with the smallest volume and the smallest exchange repulsion spheres, namely oxygen and nitrogen, which are the most electronegative atoms in the ring and, hence, exhibit the strongest charge contraction. This is in agreement with the observations made for the oxazole−argon complex, for which also a global minimum has been found in the vicinity of the O atom with a ring−Ar distance of 3.538 Å (MP2/6-31G(d); experimental value 3.485 Å; ref 14).

5. Differences between oxazole−argon and isoxazole−argon result from the different topology of the ring molecules. In the latter case, two electronegative ring atoms O and N are connected by a bond. As a consequence, the Ar atom is shifted toward the center of the NO bond thus benefiting from the polarizing power of the two rather than just one electronegative atom. This leads to the slightly larger stability of isoxazole−argon compared to the oxazole−argon. Also, its R value is somewhat smaller due to the fact that Ar feels the exchange repulsion sphere of O and N atom somewhat later when it orients itself more toward the center of the NO bond rather than directly toward the O nucleus as in the case of the oxazole−argon complex.

Acknowledgment. We thank Dr. N. Heineking, Dr. U. Kretschmer, Dr. I. Merke, Dr. J. Gripp, and the members of the Kiel group for helpful discussions. This work was supported by the Deutsche Forschungsgemeinschaft, the Fonds der Chemie, the Land Schleswig-Holstein, the Deutsche Akademische

Austauschdienst (DAAD), and the Swedish Natural Science Research Council (NFR). All calculations were done on the CRAY YMP/464 of the Nationellt Superdatorcentrum (NSC), Linköping, Sweden. The authors thank the NSC for a generous allotment of computer time.

References and Notes

(1) See, e.g.: (a) Barton, D.; Ollis, W. D. *Comprehensive Organic Chemistry, The Synthesis and Reactions of Organic Compounds, Vol. 4. Heterocyclic Compounds*; Pergamon Press: New York, 1979. (b) Wilson, C. O.; Gisvold, O.; Doerge, R. F. *Textbook of Medicinal and Pharmaceutical Chemistry*; Pitmman: London, 1966. (c) Slack, R.; Wooldridge, K. R. H. *Adv. Heterocycl. Chem.* **1965**, *4*, 107. (d) Davis, M. *Adv. Heterocycl. Chem.* **1972**, *14*, 43.

(2) Stiefvater, O. L.; Nösberger, P.; Sheridan, J. *Chem. Phys.* **1975**, *9*, 435.

(3) Stiefvater, O. L. *J. Chem. Phys.* **1975**, *63*, 2560.

(4) El-Azhary, A. A.; Suter, H. U. *J. Phys. Chem.* **1995**, *99*, 12751.

(5) For reviews on van der Waals complexes: (a) Maitland, G. C.; Rigby, M.; Smith, E. B.; Wakeham, W. A. *Intermolecular Forces*; Clarendon Press: Oxford, UK, 1981. (b) *Structure and Dynamics of Weakly Bounded Molecular Complexes*; Weber, A., Ed.; NATO ASI Series C; Reidel: Dordrecht, 1987; Vol. 212. (c) *Dynamics of Polyatomic von der Waals Complexes*; Halberstadt, N.; Janda, K. C. Eds.; NATO ASI Series B; Plenum: New York, 1990; Vol. 227. (d) Van der Waals Molecules I. *Chem. Rev.* **1986**, No. 6. (e) Van der Waals Molecules II. *Chem. Rev.* **1994**, No. 7.

(6) (a) Chalasinski, G.; Szczesniak, M. M. *Chem. Rev.* **1994**, *94*, 1723. (b) Jeziorski, B.; Moszynski, R.; Szalewicz, K. *Chem. Rev.* **1994**, *94*, 1887. (c) Hobza, P.; Selzle, H. L.; Schlag, E. W. *Chem. Rev.* **1994**, *94*, 1767. (d) Felker, P. M.; Maxton, P. M.; Schaeffer, M. W. *Chem. Rev.* **1994**, *94*, 1787. (e) Van der Avoird, A.; Wormer, P. E. S.; Moszynski, R. *Chem. Rev.* **1994**, *94*, 1975.

(7) (a) Hirschfelder, J. O.; Curtiss, C. F.; Bird, R. B. *Molecular Theory of Gases and Liquids*; Wiley: New York, 1954. (b) Hirschfelder, J. O.; Meath, W. J. *Adv. Chem. Phys.* **1976**, *12*, 3. (c) Piecuch, P.; In *Molecules in Physics, Chemistry and Biology*; Kluwer Academic Publishers: Dordrecht, 1988; Vol. 2, p 417. (d) Magnasco, V.; McWeeney, R. In *Theoretical Models of Chemical Bonding* (*Theoretical Treatment of Large Molecules and Their Interactions*); Maksic, Z. B., Ed.; Springer: New York, 1991; Part 4, p 133. (e) Buckingham, A. D. *Q. Rev. (London)* **1959**, *13*, 183.

(8) Brupbachter, Th.; Bauder, A. *Chem. Phys. Lett.* **1990**, *173*, 435.

(9) Stahl, W.; Grabow, J.-U. *Z. Naturforsch. A* **1992**, *47*, 681.

(10) Jochims, E.; Stahl, W.; Mäder, H. Unpublished results.

(11) Spycher, R. M.; Petitprez, D.; Bettens, F. L.; Bauder, A. *J. Phys. Chem.* **1994**, *98*, 11863.

(12) Kukolich, S. G. *J. Am. Chem. Soc.* **1983**, *105*, 2207.

(13) Bohn, R. K.; Hillig, K. W., II; Kuczkowski, R. L. *J. Phys. Chem.* **1989**, *93*, 3456.

(14) Kraka, E.; Cremer, D.; Spoerel, U.; Merke, I.; Stahl, W.; Dreizler, H. *J. Phys. Chem.* **1995**, *99*, 12466.

(15) MP2: Binkley, J. S.; Pople, J. A. *Int. J. Quantum Chem.* **1975**, *9*, 229. MP3: Pople, J. A.; Binkley, J. S.; Seeger, R. *Int. J. Quantum Chem. Symp.* **1976**, *10*, 1. MP4: Krishnan, R.; Pople, J. A. *Int. J. Quantum Chem.* **1978**, *14*, 91.

(16) Andresen, U.; Dreizler, H.; Grabow, J.-U.; Stahl, W. *Rev. Sci. Instrum.* **1990**, *61*, 3694.

(17) Grabow, J.-U.; Stahl, W. *Z. Naturforsch.* **1990**, *45a*, 1043.

(18) van Eijck, B. P. *J. Mol. Spectrosc.* **1974**, *53*, 246.

(19) Grabow, J.-U.; Heineking, N.; Stahl, W. *J. Mol. Spectrosc.* **1992**, *152*, 16.

(20) Gordy, W.; Cook, R. L. *Microwave Molecular Spectra*, 3rd ed.; J. Wiley and Sons: New York, 1984.

(21) Wacker, P. F.; Pratto, M. R. *Microwave Spectral Tables, Line Strength of Asymmetric Rotors*; National Bureau of Standards; Washington, DC, 1964.

(22) Chalasinski, G.; Funk, D. J.; Simons, J.; Breckenridge, W. H. *J. Chem. Phys.* **1987**, *87*, 3569.

(23) Spackman, M. A. *J. Phys. Chem.* **1989**, *93*, 7594.

(24) For a recent review on the basis set superposition problem see: van Duijneveldt, F. B.; van Dunijneveld-van de Rijdt, J. G. C. M.; van Lenthe, J. H. *Chem. Rev.* **1994**, *94*, 1873.

(25) Boys, F.; Bernardi, F. *Mol. Phys.* **1970**, *19*, 553.

(26) Kraka, E.; Gauss, J.; Reichel, F.; Olsson, L.; He, Z.; Konkoli, Z.; Cremer, D. COLOGNE94, University of Göteborg, 1994.

(27) Gauss, J.; Cremer, D. *Adv. Quant. Chem.* **1992**, *23*, 205.

(28) Stanton, J.; Gauss, J.; Watts, J. D.; Lauderdale, W. J.; Bartlett, R. J. *Aces II, Quantum Chemistry Project*; University of Florida: Gainsville, FL, 1992.

(29) (a) Kraka, E.; Cremer, D. In *Theoretical Models of the Chemical Bond, Part 2: The Concept of the Chemical Bond*; Maksic, Z. B., Ed.; Springer-Verlag: Berlin, 1990; p 453. (b) Bader, R. F. W. *Atoms in Molecules*; Clarendon Press: Oxford, UK, 1994.

(30) Loewe, S. E.; Sheridan, J. *Chem. Phys. Lett.* **1978**, *58*, 79.

(31) Spoerel, U.; Dreizler, H.; Stahl, W. *Z. Naturforsch.* **1994**, *49a*, 645.

JP960600D